

**TIGHT TOLERANCE THERMOFORMING**

*SUBMITTED TO INTERNATIONAL POLYMER PROCESSING*

HAIHONG XU AND DAVID O. KAZMER

DEPARTMENT OF MECHANICAL AND INDUSTRIAL ENGINEERING

UNIVERSITY OF MASSACHUSETTS AMHERST

AMHERST, MASSACHUSETTS 01003

Contact: Dr. David O. Kazmer

Associate Professor, Department of Mechanical & Industrial Engineering

Engineering Laboratory Building

University of Massachusetts Amherst

Amherst, MA 01003, USA

Fax: 1-413-545-1027

E-mail: [kazmer@ecs.umass.edu](mailto:kazmer@ecs.umass.edu)

## **ABSTRACT**

Tighter tolerances are becoming more prevalent as thermoforming applications are increasingly utilized in multiple component assemblies with load bearing and other functional capabilities. Analytical method is described for shrinkage predictions utilizing a thermoviscoelastic constitutive model to try and avoid costly and time consuming forming trials to determine adequacy of the mold and process. Validation experiments and sensitivity analyses were performed to understand the process behavior and estimate the accuracy of the shrinkage analysis. Design and manufacturing guidelines were then developed to facilitate tight tolerance thermoforming. While the analysis was generally capable of predicting linear shrinkage, statistical yield models indicated that improved process control and further process development is required to consistently produce thermoformed parts to tight tolerances.

## **KEYWORDS**

Thermoforming simulation, thermoviscoelasticity, shrinkage, dimensional prediction

## **1 INTRODUCTION**

Thermoforming is a widely used process to manufacture thin-walled plastic parts at relatively low cost. In this process, an exerted pressure differential rapidly deforms the softened polymer sheet to fully contact the mold surface. The formed part is usually held against the mold surface by a pressure differential to facilitate cooling and reduce final shrinkage, after which it becomes capable of sustaining the newly acquired shape. The part is then ejected and trimmed into the final product.

Compared to other polymer conversion processes, little attention has been given to the simulation and process control of thermoforming. Most commercial development processes rely on trial forming, which is costly and time consuming, to decide whether the desired geometry and

quality can be attained. Advanced technical applications challenge both the consistency of thermoforming processing technology as well as the predictive accuracy of process simulation and dimensional prediction. The objective of this paper is to support commercial applications with advanced material systems, reduce design and manufacturing cost, and gain tighter process control over the manufacturing process. Towards this objective, this paper will first develop and validate a shrinkage prediction model for use in mold design and process analysis. Then, a sensitivity analysis will be utilized to dictate process control limits and guidelines for tight tolerance thermoforming.

## **2 SHRINKAGE PREDICTION AND VALIDATION**

Shrinkage is the combined effect of structural stress accumulation due to stretching and thermal stress accumulation due to constrained cooling. A predictive shrinkage model has been developed to estimate thermoformed part dimensions given mold geometry, material properties, and processing conditions [1]. This predictive tool is necessary to estimate part shrinkage during the product development process, thereby avoiding costly tooling trials and revisions. If corrective actions are necessary during manufacturing start-up, the predictive tool can also facilitate the modification of process conditions and material properties.

The analysis methodology is shown in Figure 1. The flowchart indicates the shrinkage model includes a transient thermal analysis for temperature solution; a stretching phase analysis for inflation induced stress estimation; a post contact analysis for thermal stress and relaxation; and post-molding strain analysis after the release that supports shrinkage estimation. The development of this analysis will be briefly described.

### **2.1 Constitutive Model**

Material properties as modeled by constitutive models have a significant influence over the inflation pressure and time, numerical stability, stress profiles, and thus final solution of shrinkage. The complexity involved by adding viscosity results in numerous undetermined

material coefficients, complicated numerical schemes, and tremendous material characterization requirements. Although the visco-elastic material properties and models do not have dominant influence over thickness prediction, an efficient material model with viscosity is necessary for evaluating the stress profiles and resulting shrinkage and warpage. Significant research has been devoted to simplify the visco-elastic expression of material behavior. A more advanced form of time-strain separable model, the Kaye-Bernstein-Kearsley-Zapas (KBKZ) model of uniaxial stretching [2, 3] is becoming prevalent and has been implemented in this work as:

$$\sigma(t) = \int_{-\infty}^t \mu(t-t') \cdot h(I_1 - I_2) \cdot B(t, t') dt' \quad (1)$$

The material memory function

$$\mu(t-t') = \sum_{k=1}^N \left[ \frac{a_k}{\tau_k} \exp\left(-\frac{t-t'}{\tau_k}\right) \right] \quad (2),$$

is given by time  $t$ , the time variable in relation to  $t'$ , and the material dependent parameters  $a_k$ ,  $\tau_k$ .

For biaxial stretching,  $i = 1, 2$ , equation (1) can be extended to the following form

$$\sigma_i(t) = h(t)[\lambda_i^2(t) - \lambda_3^2(t)]G(t) + \int_0^t \mu(t-t')h(I_1, I_2)[\lambda_i^2(t-t') - \lambda_3^2(t-t')]dt' \quad (3)$$

where

$$G(t) = \int_{-\infty}^0 \mu(t-t')dt' \quad (4)$$

## 2.2 Thermal Analysis

Thermal analysis is used to derive the temperature history at each location in the polymer sheet, which is necessary for temperature dependent stress accumulation and relaxation. A finite difference method was used to model the temperature distribution through the thickness of the polymer and mold with convective boundary conditions. Although large time steps or a small number of elements in the mesh will degrade the accuracy of the solution obtained with the

implemented implicit solver, it will not affect the stability. Gauss-Seidel iteration [4] was used instead of matrix inversion in order to optimize the solution speed.

### 2.3 Stress Analysis of the Inflation Phase

The mechanically accumulated stress was estimated from the sheet inflation stage that resulted in a known thickness distribution of the thermoformed part. The stretching history is highly dependent on the geometry of the mold, forming pressure, temperature and other factors. A general analytical solution of the stretching history is difficult to derive for complex geometry because of its dependency with location. It is observed in thermoforming trials that the polymer sheet contacts the closest flat surface of the mold first with minimum stretching, while other areas of the sheet continue to stretch into the corners until the part is fully formed. In many thermoforming applications, a strong vacuum or pressure assist is used to ensure that the sheet contacts small features of the mold. The large pressure difference between two sides of the sheet purposely drives the sheet stretching much more quickly than inflation under the kinetic equilibrium. To simplify the analytical solution, the entire polymer sheet is assumed to be expanding at a constant stretch rate until it contacts the mold, i.e.

$$\dot{\varepsilon} = const \quad (5)$$

The stress load resulting from the pressure difference on an expanding spherical membrane can be estimated as [4, 5]

$$\sigma \approx \frac{PR}{2b} \quad (6)$$

where  $P$  is the applied pressure,  $R$  is the expanding radius, and  $b$  is the membrane thickness. The elastic liquid response of polymer to the applied stress has the form,

$$\sigma = \eta_e \cdot \dot{\varepsilon} \quad (7)$$

where  $\eta_e$  is the apparent viscosity of the polymer flow. Considering the different conditions at the beginning and the end of the stretching, the average stretch rate can be estimated as,

$$\dot{\varepsilon} = \frac{P}{2\eta_e} \left[ \frac{R_0}{2b_0} + \frac{R_{cor}}{2b_{cor}} \right] \quad (8)$$

where  $R_0$  represents the estimated radius of the inflated sheet when it initially contact the mold, and  $R_{cor}$  represents the radius of the smallest feature of the part and the corresponding thickness after stretching. The biaxial extension of the polymer sheet coincides with contraction in the thickness direction [6, 7]. By assuming material incompressibility and homogeneous deformation, the Hencky strain in the thickness direction is given by

$$\varepsilon = \ln(b/b_0) \quad (9)$$

where  $b$  is the sheet thickness as a function of time. The strain rate is,

$$\dot{\varepsilon} = \frac{d\varepsilon}{dt} = \dot{b}/b \quad (10)$$

The corresponding biaxial extension under as incompressible assumption becomes,

$$\dot{\varepsilon}_b = -\dot{\varepsilon}/2 = -\frac{1}{2} \dot{b}/b \quad (11)$$

The above reasoning relates the in-plane strain and strain rate directly to the thickness variation across the polymer sheet. The final thickness distribution is stable and easy to obtain either experimentally or numerically. Employing the measured thickness distribution, the stress and strain distributions at the end of the stretching phase can be estimated using the described models.

#### 2.4 Stress Analysis in the Cooling Stage

The stretching stops when the polymer sheet fully contacts the mold. As the sheet temperature drops, the part gains stiffness and capability to sustain the shape of the mold. The strain involved in the cooling stage is negligible compared to that in the stretching stage, and is

readily estimated using elastic material models. However, the significant temperature drop and the relatively long time span imply that the thermal effect on relaxation and shrinkage behavior cannot be overlooked. The stress accumulation during the cooling stage is mostly thermally induced. After the part is ejected, the residual stress will be released and subsequently cause shrinkage and warpage.

Taking into account the stress relaxation and the variation of Young's Modulus over time, a numerical scheme is derived as follows. When the part is constrained by the mold surface, the thermal residual stress increment without relaxation at time  $t$  is given by

$$\Delta\sigma(t) = (\alpha - \alpha_{mold}) \cdot [T(t) - T(t + \Delta t)] \cdot E(t) \quad (12)$$

The stress can be evaluated from following iterations,

$$\sigma(t + \Delta t) = [\sigma(t) + \Delta\sigma(t)] \cdot g(\Delta t, T(t)) \quad (13)$$

$$\sigma(t_{cntc}) = \sigma_{cntc} \quad (14)$$

where  $g(\Delta t, T(t))$  is the relative relaxation modulus at temperature  $T(t)$  for time span  $\Delta t$ . The stress at the point when the part is mechanically released from constraint,  $\sigma(t_{rels})$ , can be derived using the equations above and substituted into the shrinkage model discussed in previous sections. The shift function for temperature is assumed to the standard WLF shift function.

## 2.5 Shrinkage Analysis upon Ejection

Under mechanical constraint of the sheet common for male forming or pressure vacuum holding of the parts during the cooling phase, the thermal stress will be accumulated and experience significant relaxation before released as strain. Upon release from the mold, the accumulated residual stress will cause shrinkage in the thermoformed part, followed by additional thermal contraction as the part cools to the end-use temperature. An analytical model was developed to include the constraint effects in the cooling phase. The free shrinkage in the  $x$  direction, from position  $x_{min}$  to position  $x_{max}$  can be estimated as:

$$S = \int_{x_{\min}}^{x_{\max}} \{ \alpha [T_{rels}(x) - T_{end}] - \alpha_{mold} (T_{mold} - T_{end}) \} dx + \int_{x_{\min}}^{x_{\max}} \frac{\sigma(t_{release})}{E(x, T_{release})} dx \quad (15)$$

where  $T_{release}$  and  $t_{release}$  are the temperature and the time when the part is no longer constrained by the mold surface,  $\alpha$  and  $\alpha_{mold}$  are the thermal expansion coefficient of the polymer and the mold,  $T_{end}$  is the end use temperature of the thermoformed part,  $\sigma_{acc}(x)$  is the  $x$  direction stress component at position  $x$  accumulated when the sheet fully contacts with mold, and  $E(x)$  is the location dependent modulus at the time of part ejection. For male molding, the release happens when the part is ejected. For female molding, the release happens when the pressure or vacuum holding of the part stops. For parts with complex features, the release can be governed by either or both of the two scenarios. In some case, the holding pressure or vacuum is not sufficient to maintain the contact with the mold surface. The stress threshold which may trigger the release can be estimated as,  $\sigma_{release} = P \cdot f_s$ , where  $P$  is the holding pressure, and  $f_s$  is the static friction coefficient.

### 3 SHRINKAGE VALIDATION

Validation was performed to verify the described assumptions and models. Table 1 contains all the material properties and process settings required by the analysis. A commercial thermoforming finite element analysis (FEA) was used to obtain the thickness distribution input for the shrinkage simulation [3]. The FEA utilizes the KBKZ model and specializes in simulating the inflation of thermoforming, predicting the wall thickness distributions and temperature distributions according to the stretching rate of the part and geometry of the mold.

#### 3.1 Process Description

The thermoforming process has been studied through investigations into machine setup parameters and real-time data acquisition of thermoforming trials. The thermoforming process is a combination of a complex series of events, including the clamping and removal of the polymer

sheet, the shuttling of sheet from station to station, the open and closing of the mold platens, the exertion of pressure and vacuum, the air-assist part ejection, and the on/off of the cooling fans. This sequence of events can be programmed into a sophisticated thermoforming machine with position, temperature, pressure and time control to perform specific thermoforming tasks.

Figure 2 summarizes the critical events that occurred during a typical female forming cycle with a controlled time sequence. The duration of each event is marked by the solid line. The dotted lines demonstrate the movement of the top and bottom platens, where the mold and the pressure box were mounted. The polymer sheet is heated up by the oven, and then shuttled to the forming station at the signal of the machine infrared sensor inside the oven. After the mold is engaged, pressure or vacuum is applied to shape the polymer sheet into the mold with respect to specific forming technique in use. The mold is then completely opened and the part ejected at the end of the forming cycle.

The timer in the thermoforming machine starts to record the forming cycle time at the moment when the position sensor in the forming station is triggered by the sheet arrival. The actual mold cycle time refers to the in-mold cooling time, and can be retrieved experimentally. A male molding application would assume the cooling time of the part is equal to the machine specified in-mold cooling time. However, a female molding application should assume a cooling time equal to the pressure holding time. Caution needs to be exercised when interpreting shrinkage estimates on predominantly female molds with some male features.

Several infrared sensors were located in the oven and pressure box to monitor the sheet temperature and provide actuation signals. It was discovered that the actual sheet temperature at forming is several degrees cooler than the machine setting temperature, which triggers the shuttle movement of the sheet. Moreover, the actual pressure on the sheet during forming was found to differ significantly from the machine settings [1]. In fact, the sheet is completely formed before the pressure reaches its maximum. Thus, the pressure to be used in the modeling should be obtained from the pressure sensor trace.

### 3.2 Design of Experiments

To determine the effect of processing parameters on the final shrinkage of the thermoformed part, a  $2^4$  full-factorial design of experiments (DOE) has been performed for female mold forming using a common thermoforming grade of ABS. Formed from a 3 mm thick sheet, the part is fairly large (1500 by 600 mm) with part thicknesses ranging from 1 to 2.5 mm. Significant process variables that were considered are sheet heating temperature, forming pressure, mold coolant temperature, and in-mold cooling time. The mean level for each controlled variable is determined by trial forming. The upper and lower levels of each variable are kept inside the forming process window to produce parts with adequate quality. As shown in Table 2, sixteen runs were conducted on each mold with two or three replicates per run. The main effect and variance analysis were then performed with MiniTab, a statistics analysis program.

Linear shrinkage was determined by comparing the three dimensional CAD model of the mold contact surface at room and molding temperatures to that of the part surface at room temperature. The measurement and three-dimensional CAD modeling was performed by a Faro Arm (Stuttgart, Germany) as the location capture device with a precision of 0.01 mm. The CAD model has been built for the mold as well as certain parts for the DOE runs. Sample CAD models are shown in Figures 3.

### 3.3 Shrinkage Results

Because of the extreme cost in accurately measuring the formed parts, only those DOE runs that were believed to encompass the shrinkage range were measured. The observed and predicted shrinkage results for the female paint tray at five DOE runs and nominal conditions are compared in Table 4. Referring to Figure 3, the centerline dimension in the longer direction was denoted as  $X$ , and the dimension across the bottom edges of the part are marked as  $Y1$  and  $Y2$  for deeper end and shorter end respectively.

These results indicate that the shrinkage estimates provided by the shrinkage analysis were within 0.1% of the absolute measured shrinkage. In fact, the average observed shrinkage across all observations (five runs and three dimensions) was 0.53%, which is only 0.02% larger than the overall predicted average of 0.51%. Inasmuch as absolute error of the shrinkage prediction should be minimized, however, the relative sensitivity of the prediction to changes in critical process conditions should also be accurate. Figure 4 plots the estimated main effects of sheet temperature, forming pressure, cycle time, and mold coolant temperature with respect to the observed and predicted shrinkage.

Generally, the sensitivity of the thermoformed part shrinkage to changes in the process settings have been well captured by the analysis. Sensitivity prediction is extremely important since the observations indicate that the shrinkage can be adjusted approximately 0.1% through the machine settings. Thus, some dimensional errors can be corrected at the point of processing by utilizing the analysis to indicate the direction of necessary changes. The sensitivity analysis of the main effects shows that the described shrinkage model is very sensitive to the setting of cycle time and mold temperature. Interestingly, the high sensitivity of the shrinkage may also explain the observed part-to-part variation and indicates the need for tighter control on these parameters.

The sheet temperature response of the shrinkage analysis is slightly less sensitive than the observed response from the experimental design. This could be due to erroneous modeling of material relaxation at higher temperatures, which is difficult to characterize. Alternatively, there is usually a 2 to 20 second delay between the sheet removal from the oven and the start of forming, which could significantly influence the sheet temperature at stretching. However, the actual temperature at stretching is hard to determine by infrared sensor due to sheet movement and delay in sensor response.

The shrinkage analysis does not predict the effect of pressure compared to the observed response. An investigation of the pressure history during the stretching phase reveals that the forming pressure stated by the machine settings is not exerted onto the polymer sheet for the

entire processing time span. Specifically, the recorded pressure history indicates that the increase of the forming pressure from zero to the specified setting usually requires 5 to 10 seconds to complete. This machine response is poor considering that the stretching of the sheet generally stops within a small fraction of a second.

The shrinkage analysis independently estimates the start and ending pressure of the stretching phase, thus the actual pressure simulated is much lower than the nominal machine settings. However, there is still some potential of over predicting the exerted stress by utilizing the unmodified machine settings, thereby increasing the sensitivity of pressure response. Given these findings, the characterization of the actual pressure exerted onto the stretching sheet requires further validation, and more sophisticated pressure estimation methods may enable higher levels of predictive accuracy.

#### **4 TIGHT TOLERANCE THERMOFORMING**

The proposed tight tolerance thermoforming methodology is shown in Figure 5. The methodology begins with the product specification, which has been developed to satisfy the customer requirements. It is vital that the development team understand the specifications so that they may develop an adequate material, mold, and process design.

The following tight tolerance guidelines are intended to enable a design that requires no re-design, i.e. that results in adequate quality upon production start-up, or that can be sufficiently improved through modifications to machine settings only. As such, guidelines for design and processing in tight tolerance thermoforming are next discussed.

##### **4.1 Design Guidelines**

SPI injection molding guidelines provide a general allowance of 0.2% nominal part length for standard tolerances [8], while tolerances below 0.1% of the nominal length are generally considered tight. For example, if a dimension was specified as 100 cm, a standard tolerance for that dimension would be specified as  $100.00 \pm 0.20$  cm.

Tolerances for thermoformed parts have typically been looser than SPI guidelines for two reasons. First, thermoformed parts have a much higher length to thickness ratio than molded or extruded parts. The investigated part in this example, for instance, has a length to thickness ratio of approximately 1000:1, compared to typical ratios of 100:1 for injection molding and extrusion. Thus, thermoformed parts are significantly more compliant and can be manipulated into necessary geometries at the point of end-use. Second, thermoforming applications have not historically required the specification of tight functional tolerances. Functional tolerances are typically specified due to mating of multiple contact surfaces in an assembly or rigid positioning of sub-assemblies. Since thermoformed parts have not been used extensively in rigid assemblies, tight tolerances have not been widely utilized.

However, advanced thermoforming applications are more frequently requiring tighter dimensional tolerances. The exact quality of thermoformed parts cannot be known precisely beforehand, and thus the design team faces the likelihood that design and process changes are necessary. Tight tolerance thermoforming requires precise control of process variables (low noise) as well as accurate control of the process mean (low uncertainty). Figure 5 demonstrates the difference in the concept of noise and uncertainty. Target A has little production variation, but a large fixed offset. Target B has a small mean offset, but a large variation, representing a centered design with a process that is out of control. Finally, target C has both a small production variation and a small offset, representing the desired outcome for tight tolerance products.

There are three critical guidelines for tight tolerance design: 1) specify few tolerances, 2) specify loose tolerances, and 3) cut steel safe. First, typical part drawings may specify dozens or even hundreds of dimensions. However, only a few of dimensions are typically critical to function and can be used as an overall estimator of part quality. As such, specifying fewer critical tolerances not only provides greater focus for the development team, but also provides fewer conflicting objectives for the manufacturing team while trying to start-up the production process.

It has been estimated that a reduction from 10 to 3 specified tolerances can improve production yields by 50%, enabling an infeasible process to become economically feasible [9].

Second, specification of wider tolerances can ensure that critical to function dimensions can be consistently maintained. Tight tolerances can be specified at 0.10% per length (or tighter) while other dimensions should be toleranced at 0.40% per length. Specifically, in-plane dimensions should be tightly toleranced at the expense of out-of-plane dimensions. For example, critical dimensions could include the point-to-point distance along the bottom of the part, or the depth dimensions around the edges of the part shown in Figure 3. The physical thermoformed part is extremely rigid along these lengths, and any dimensional changes would require significant material strain during end-use. By comparison, the point-to-point distance across the top of the part is an out-of-plane dimension that is highly compliant and can be readily manipulated at the time of assembly. The relationship between tightness of tolerances will be quantified in the next section.

Finally, most mold and tool designers know that they should cut “steel safe.” However, mold designers should reflect on the likely center and flexibility of the manufacturing process. Simulations can be effectively utilized to estimate the mean and sensitivity of strength, thickness, and shrinkage to material, mold, and process parameters. Small corrections in part dimensions can be corrected through process changes if necessary, while larger corrections should be corrected through modest material removal from the mold.

#### 4.2 Manufacturing Guidelines

The objective of this section is to provide some quantitative control limits for control of the thermoforming process. For a normally distributed process, the number,  $n$ , and range,  $\pm\delta$ , of specified tolerances will directly effect the production yield of acceptable thermoformed parts.

This yield,  $\Psi$ , can be evaluated as the integral across the joint probability density function for each of the specified part dimensions,  $y_k$ :

$$\Psi = \int_{y_1-\delta_1}^{y_1+\delta_1} \int_{y_2-\delta_2}^{y_2+\delta_2} \cdots \int_{y_n-\delta_n}^{y_n+\delta_n} pdf(y_1, y_2, \dots, y_n) dy_1 dy_2 \dots dy_n \quad (16)$$

In reality, the characterization of part length distributions requires extensive sampling across the production window. The characterization of the joint probability density function is impractical. However, let us assume that a production yield,  $\Psi$ , of 98% is acceptable. Assuming that the process is centered and each specified dimensional tolerance independently contributes equally to the number of defects, then the probability,  $p$ , of a dimension being out of specification is [10]:

$$p = \Psi^{1/n} \quad (17)$$

For an application with three critical dimensions, the required probability,  $p$ , of a dimension being acceptable is 99.3%. This probability is closely coupled to the process capability index,  $Cp$ :

$$Cp = \frac{USL - LSL}{6\sigma} \Rightarrow \sigma = \frac{USL - LSL}{6Cp} \quad (18)$$

where  $USL$  and  $LSL$  indicate the upper and lower tolerances for the specified dimension, and  $\sigma$  represents the standard deviation of dimension. The probability of 99.3% corresponds to a process capability,  $Cp$ , of 1.4. Thus, the required standard deviation on the length may be calculated directly from the specified tolerances, number of tolerances, and desired process capability. If a tolerance of 0.10% is to be maintained for three dimensions with a 98% production yield, then the allowable standard deviation on length during the production process is 0.012%.

It should be noted that the desired standard deviation on length directly defines the allowable process control limits during production. The relationship for output variance,  $V(y)$ , resulting from process variance,  $V(x_j)$ , can be assessed through the moment matching method [11]:

$$V(y) = \sum_{j=1}^m V(x_j) \frac{dy}{dx_j} \quad (19)$$

It is clear from eq. 19 that the processing variables will contribute unequally to the production variance in proportion to the magnitude of the sensitivity. However, a guideline for the control limits of each processing variable can be estimated by assuming that each process variable contributes equally to the decline in the production yield, i.e. each processing variable is given an allowance of production variation. Using the relations from the sensitivity analysis and validation, the allowable process variances are estimated in Figure 4. The results are summarized in Table 4.

The results indicate that tight control on all process variables is necessary if tight tolerances are going to be consistently produced in the thermoforming process. Specifically, the results denote that current control technologies on sheet temperature and inflation pressure are likely sufficient. However, current control techniques for cooling time and mold temperature control are inadequate. In both experimental and production forming facilities, it was found that the cooling time may vary wildly (dependent upon process set-up and operator integrity) but should be the most tightly controlled variable. Mold temperature variation, and the effect that cycle time variation has on mold surface temperature, has also been found to be a significant source of production variation that can render tight tolerance thermoforming infeasible.

## 5 CONCLUSIONS

Tighter tolerances are becoming more prevalent as thermoforming applications are increasingly utilized in multiple component assemblies with load bearing and other functional capabilities. Thermoformed parts are subject to large dimensional variation depending on the mechanical constraints and residual stresses, which makes the measurement and interpretation of measured shrinkage very difficult. Design and manufacturing guidelines for tight tolerance thermoforming have been provided, based on a validated thinning and shrinkage analysis that utilizes a thermoviscoelastic constitutive model. In actual production environment, parts of

complex geometry (with both male and female features) are potentially beyond the scope of current analysis, which assumes the part has only male or female features.

The results of this paper show that very tight tolerances are infeasible in most production thermoforming environments given the level of process control required to minimize process variation. Separating the part compliance from the measured shrinkage, and utilizing part bending to control critical dimension by pre-stressing the assembly will be a future area of interest in tight tolerance thermoforming. The effect of three-dimensional bending and warpage, the trimming of the part, the in-plane stress variation of heavy gage thermoforming, and the heat profiling are other influential aspects in thermoforming that require further exploration. If further validation proves the capability of the model for varying material behaviors, process settings, part and model designs, it would be attractive to develop more sophisticated software implementing the shrinkage model to assist new product development. One approach is to implement the methodology directly within the FEA packages for general thermoforming applications, and utilize the FEA solution of thickness, principle stretching, and post-contact stress to evaluate the shrinkage in three-dimensions. Another approach is to integrate the shrinkage model to CAD/CAM packages, where the thickness measurement information can be stored. Shrinkage estimation can be obtained from evaluating the CAD geometry models, and could be very informative to the design engineers during the early stages of product development.

## BIBLIOGRAPHY

- [1] H. Xu and D. O. Kazmer, "Thermoforming Shrinkage Prediction," *Polymer Engineering and Science*, vol. to appear., 2001.
- [2] R. I. Tanner, *Engineering rheology*, 2nd ed. Oxford ; New York: Oxford University Press, 2000.
- [3] K. Kouba and P. Novotny, "Computer Simulation of Thermoforming Process- The Role of Material Behavior," in *Thermoforming Quarterly*, vol. Fall, 1998, pp. 13.
- [4] S. I. Krishnamachari, *Applied Stress Analysis of Plastics, A Mechanical Engineering Approach*. New York, NY: Von Nostrand Reinhold, 1993.

- [5] J. L. Throne, "Guidelines for thermoforming part wall thickness," *Polym.-Plast. Technol. Eng.*, vol. 30, pp. 685-700, 1991.
- [6] C. W. Macosko, *Rheology : Principles, Measurements, and Applications*. New York, NY: VCH, 1994.
- [7] S. Chatraei, C. W. Macosko, and H. H. Winter, "Lubricated Squeezing Flow: A New Biaxial Extensional Rheometer," *Journal of Rheology*, vol. 25, pp. 433-443, 1981.
- [8] M. C. Beris, *Standards and Practices of Plastics Custom Molders*, 5 ed: Van Nostrand Reinhold Co., New York., 1991.
- [9] D. O. Kazmer, "Best Practices for Injection Molding," *Journal of Injection Molding Technology*, vol. 1, pp. 10-17, 1997.
- [10] A. Papoulis, *Probability, Random Variables, and Stochastic Processes*, 3rd edition ed: McGraw-Hill, 1991.
- [11] J. L. Devore, *Probability and Statistics for Engineering and the Sciences*, 4th edition ed: Wadsworth, 1995.

## List of Tables and Figures

*Table 1: Required input parameters of the shrinkage prediction software*

*Table 2: 2<sup>4</sup> full-factorial design of thermoforming experiments*

*Table 3: Comparison of observed and predicted shrinkage of parts from female mold*

*Table 4: Comparison of allowable and estimated thermoforming and process variance*

*Figure 1: Shrinkage Analysis Methodology*

*Figure 2: Event chart of a male thermoforming trial*

*Figure 3: CAD models of female mold and part*

*Figure 4: Estimated sensitivity of shrinkage to process changes*

*Figure 5: Tight tolerance thermoforming methodology*

*Figure 6: Production noise vs. error offset*

*Table 1: Required input parameters of the shrinkage prediction software*

Material properties	Process condition	Geometry
Thermal and mechanical properties of sheet (E(T), CTE, Tg ...) Material model parameters (KBKZ/Time-strain separable) Mold material thermal properties Coolant thermal properties	Sheet temp. Mold temp. End use temp. In mold cooling time Holding time Forming pressure	Mold configuration and geometry Original thickness of the sheet Final thickness distribution of part

Table 2:  $2^4$  full-factorial design of thermoforming experiments

Run	Sheet Temp	Pressure	Cycle Time	Mold Temp
1	330	10	40	140
2	350	10	40	140
3	330	30	40	140
4	350	30	40	140
5	330	10	120	140
6	350	10	120	140
7	330	30	120	140
8	350	30	120	140
9	330	10	40	185
10	350	10	40	185
11	330	30	40	185
12	350	30	40	185
13	330	10	120	185
14	350	10	120	185
15	330	30	120	185
16	350	30	120	185

Table 3: Comparison of observed and predicted shrinkage of parts from female mold

		Nominal Dimension					
		X=1494.41		Y1=627.23		Y2=654.99	
		Observed	Predicted	Observed	Predicted	Observed	Predicted
Run 3	(mm)	8.65	8.52	4.25	3.47	3.23	3.44
	(Rate)	0.58%	0.57%	0.68%	0.55%	0.49%	0.53%
Run 4	(mm)	8.75	8.55	3.95	3.39	2.09	3.49
	(Rate)	0.59%	0.57%	0.63%	0.54%	0.32%	0.53%
Run 13	(mm)	8.19	7.48	4.2	3.56	3.94	3.5
	(Rate)	0.55%	0.50%	0.67%	0.57%	0.60%	0.53%
Run 14	(mm)	8.32	7.46	3.96	3.45	3.28	3.45
	(Rate)	0.56%	0.50%	0.63%	0.55%	0.50%	0.53%
Run 15	(mm)	7.88	7.48	3.59	3.57	3.12	3.57
	(Rate)	0.53%	0.50%	0.57%	0.57%	0.48%	0.55%

*Table 4: Comparison of allowable and estimated thermoforming and process variance*

Process Parameter	Allowable Range	Variance Contribution
Sheet Temperature	$\pm 1.4$ C	25%
Inflation Pressure	$\pm 0.07$ atm	25%
Cooling Time	$\pm 0.08$ sec	25%
Mold Temperature	$\pm 0.12$ C	25%

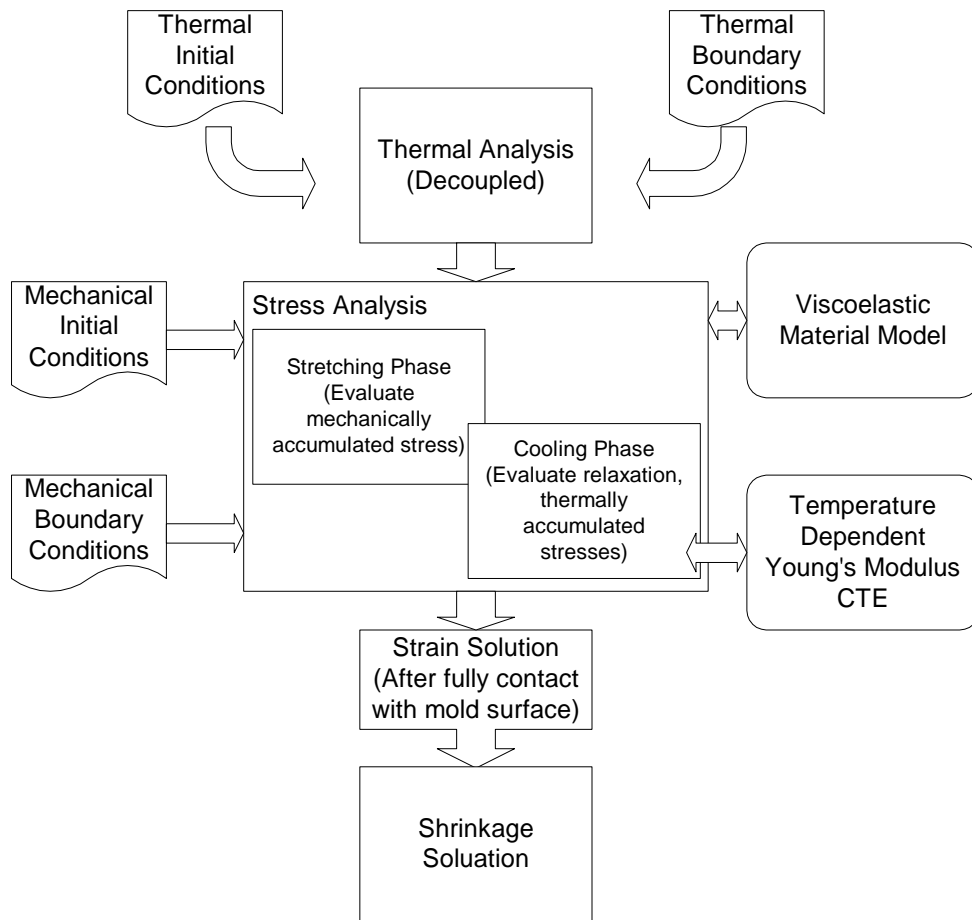


Figure 1: Shrinkage Analysis Methodology

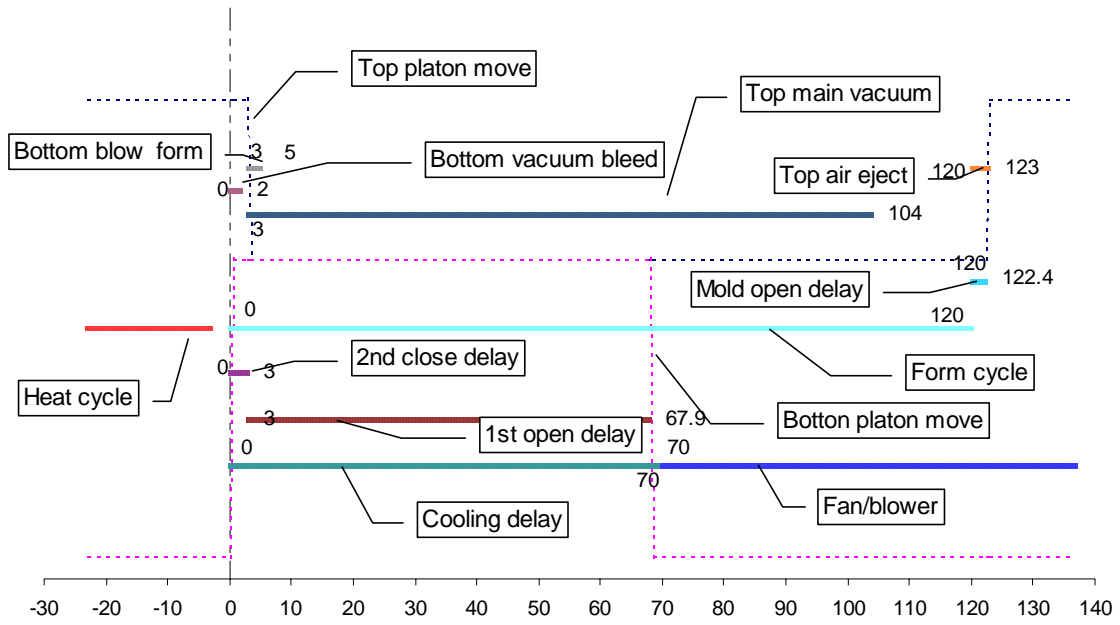
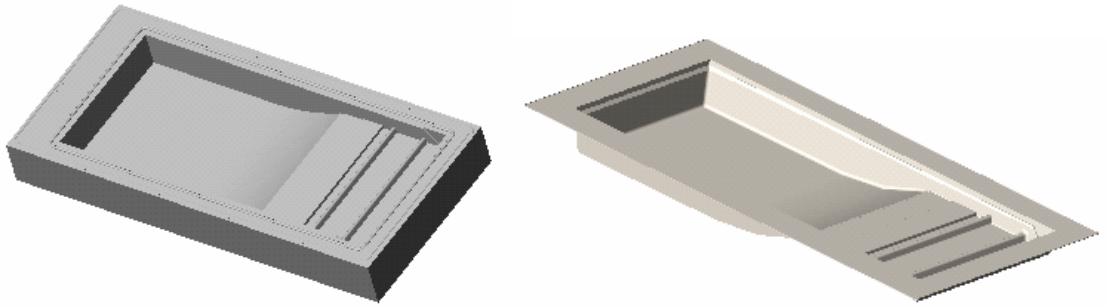


Figure 2: Event chart of a male thermoforming trial





*Figure 3: CAD models of female mold and part*

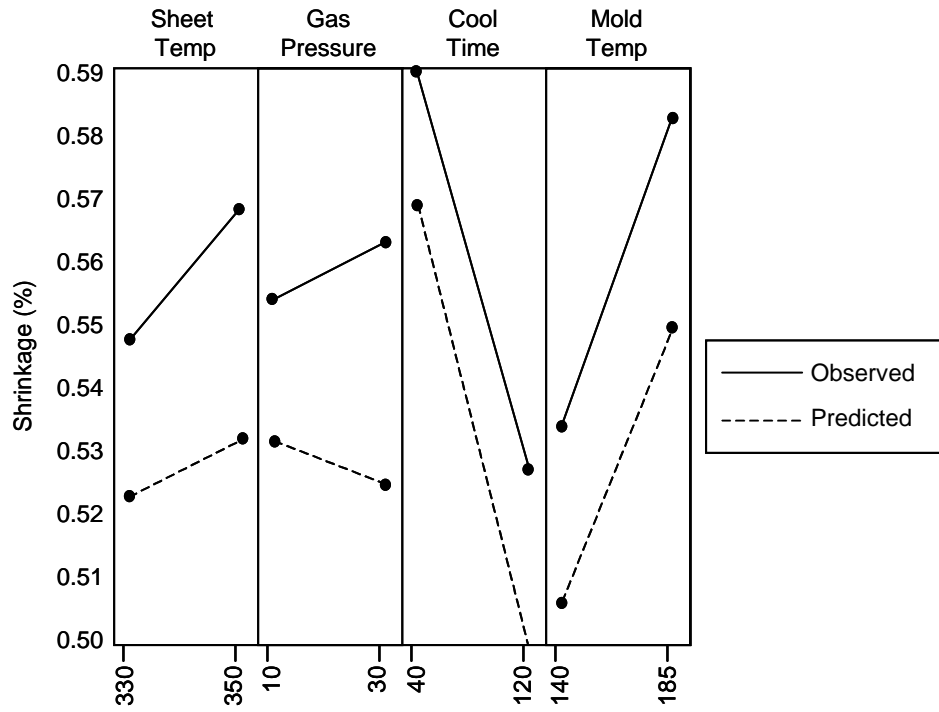


Figure 4: Estimated sensitivity of shrinkage to process changes

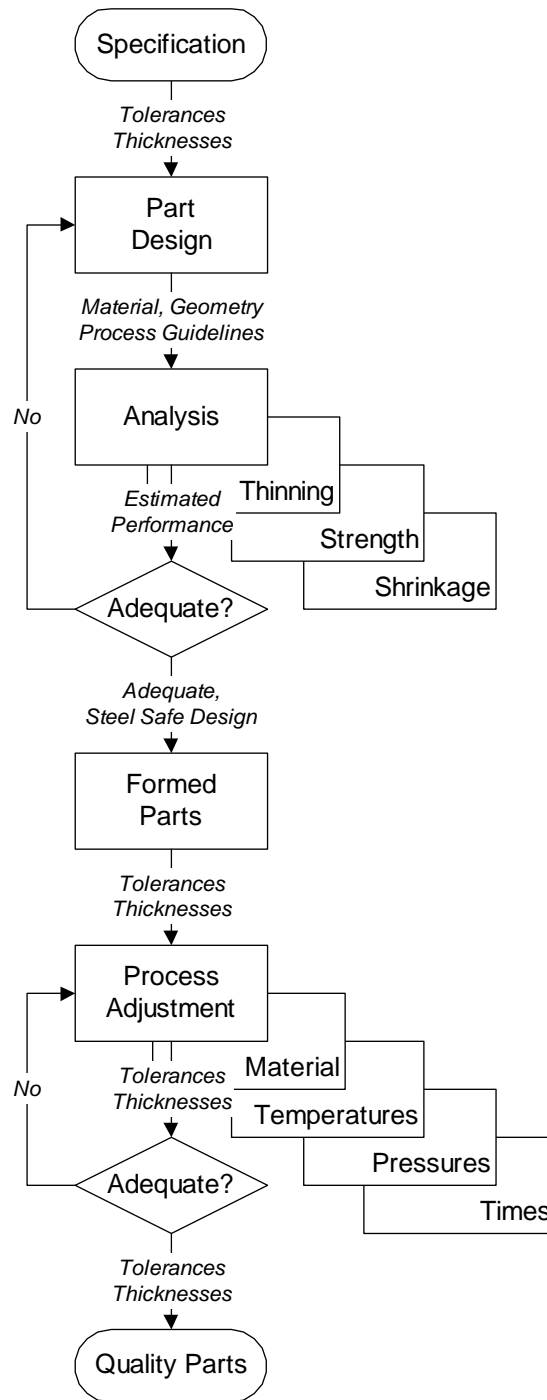
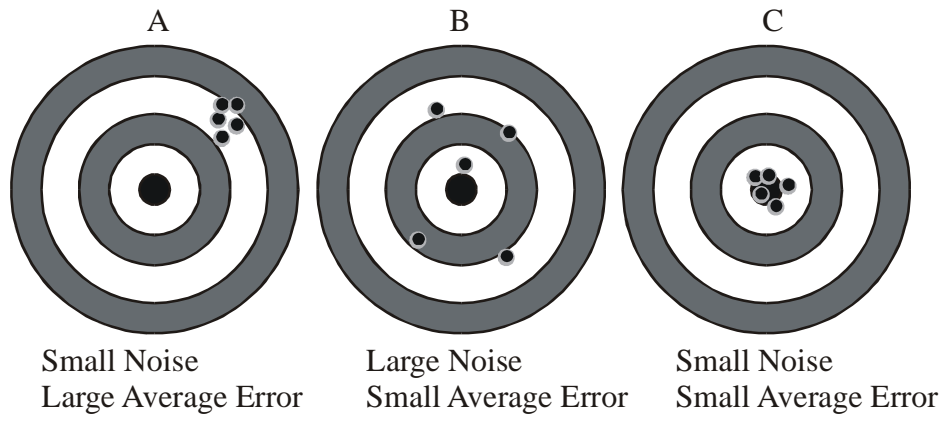


Figure 5: Tight tolerance thermoforming methodology



*Figure 6: Production noise vs. error offset*